

## 1. Selected Figures for Stellar SEDs

J. Cohen, Nov 2007, Caltech (for AY 123)

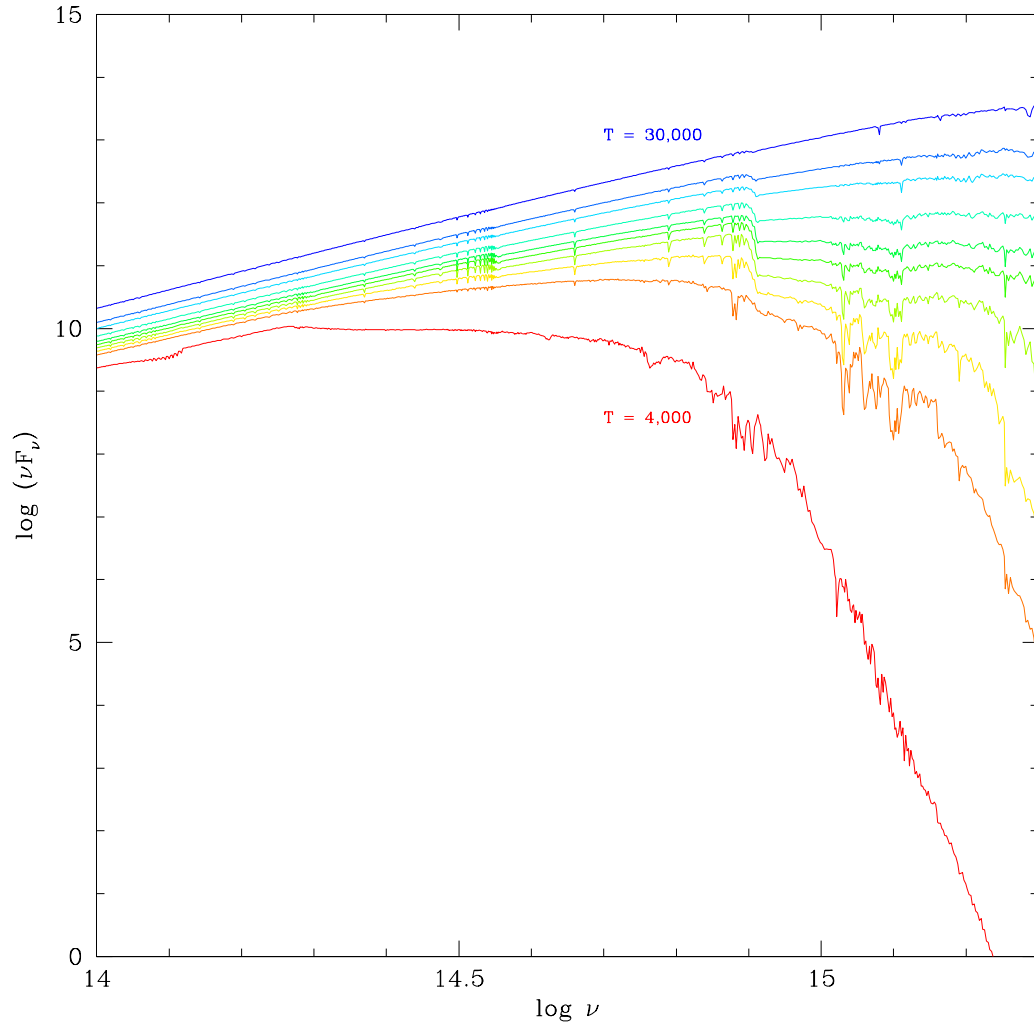


Fig. 1.— SEDs from the Kurucz model atmosphere grid for Solar metallicity giants.

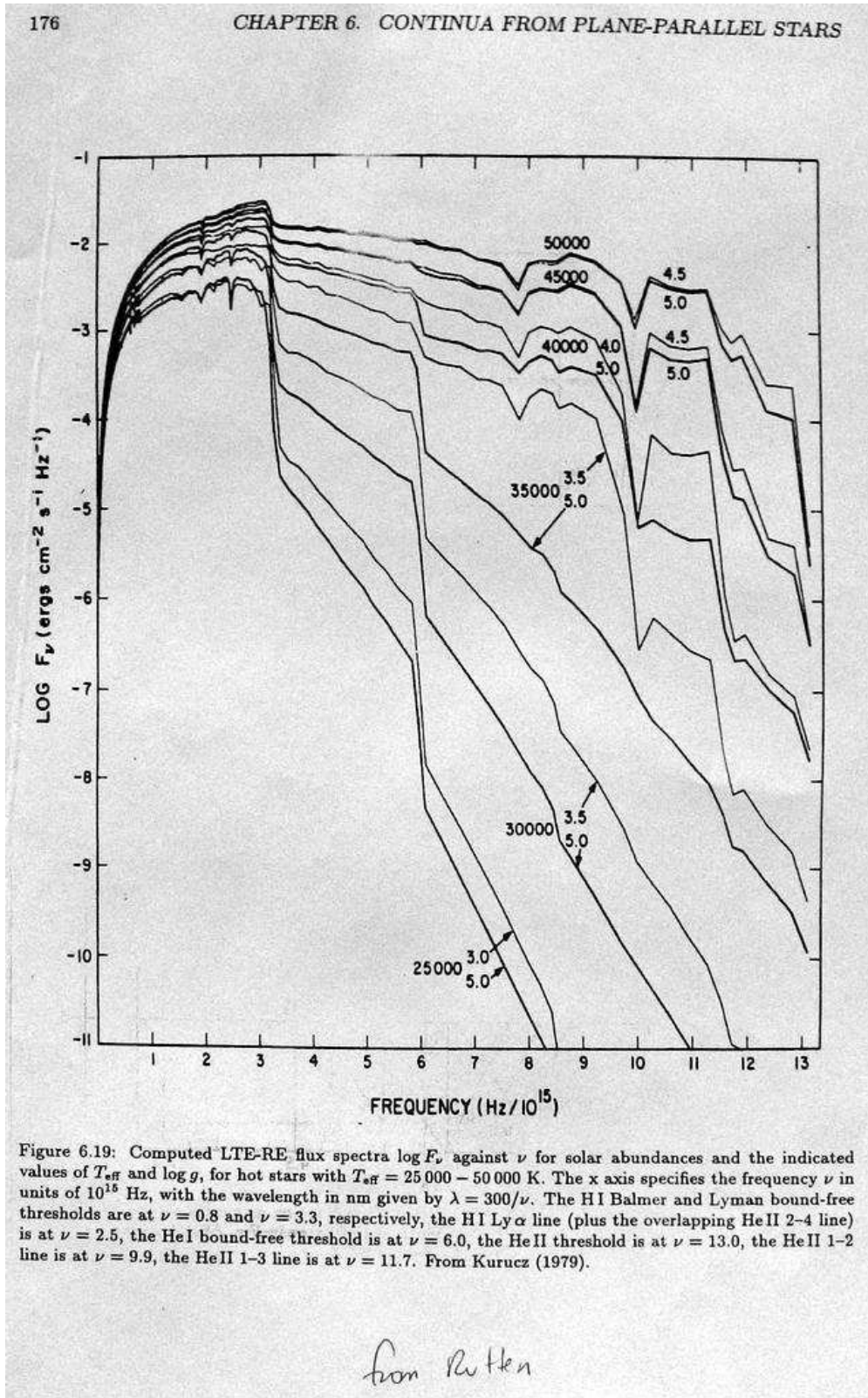


Fig. 2.— SEDs from the Kurucz model atmosphere grid for high  $T_{\text{eff}}$  Solar metallicity main sequence stars. (Fig. 6.19 from Rutten)

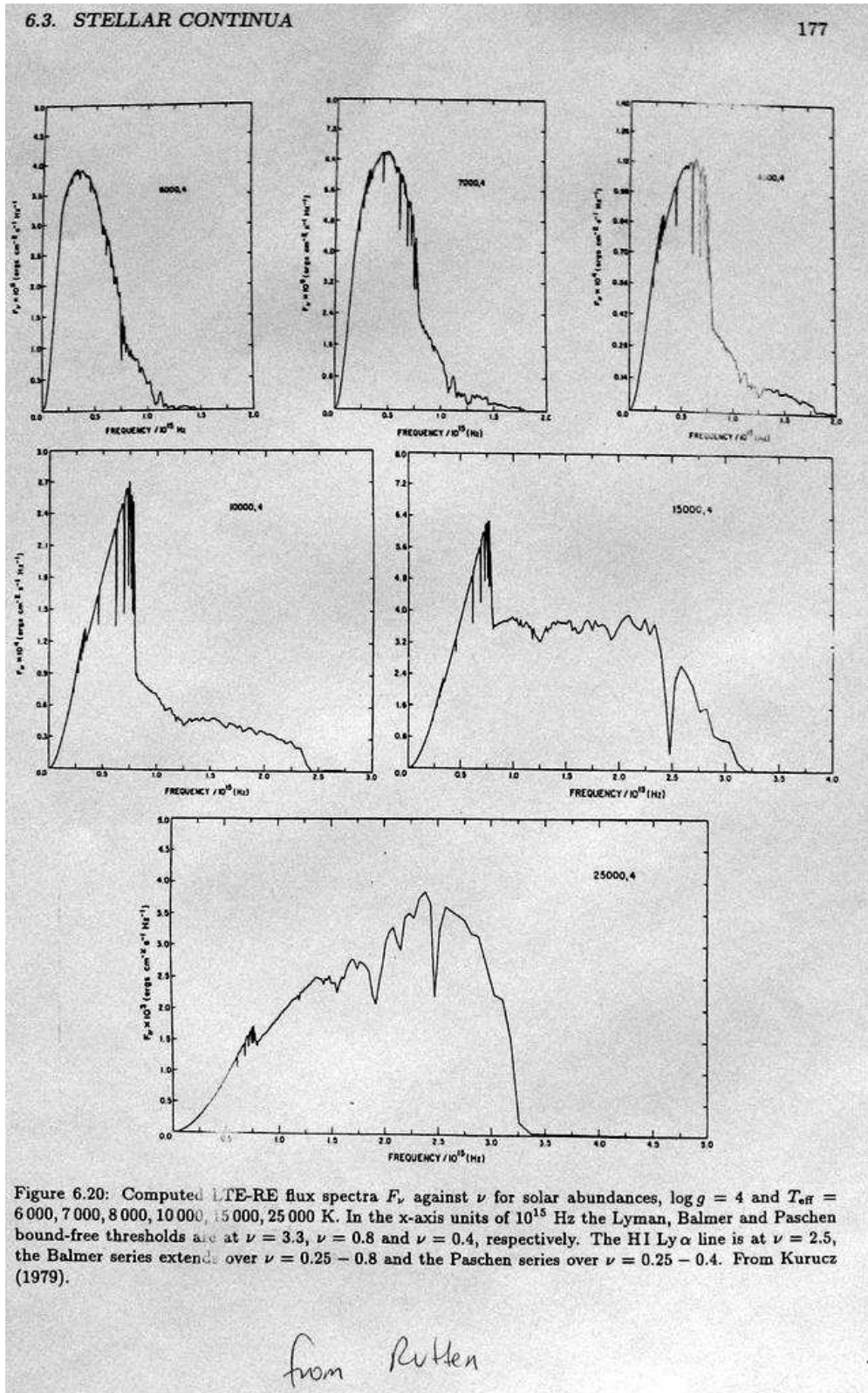


Fig. 3.— SEDs from the Kurucz model atmosphere grid for a wide range of  $T_{\text{eff}}$  Solar metallicity main sequence stars. (Fig. 6.20 from Rutten)

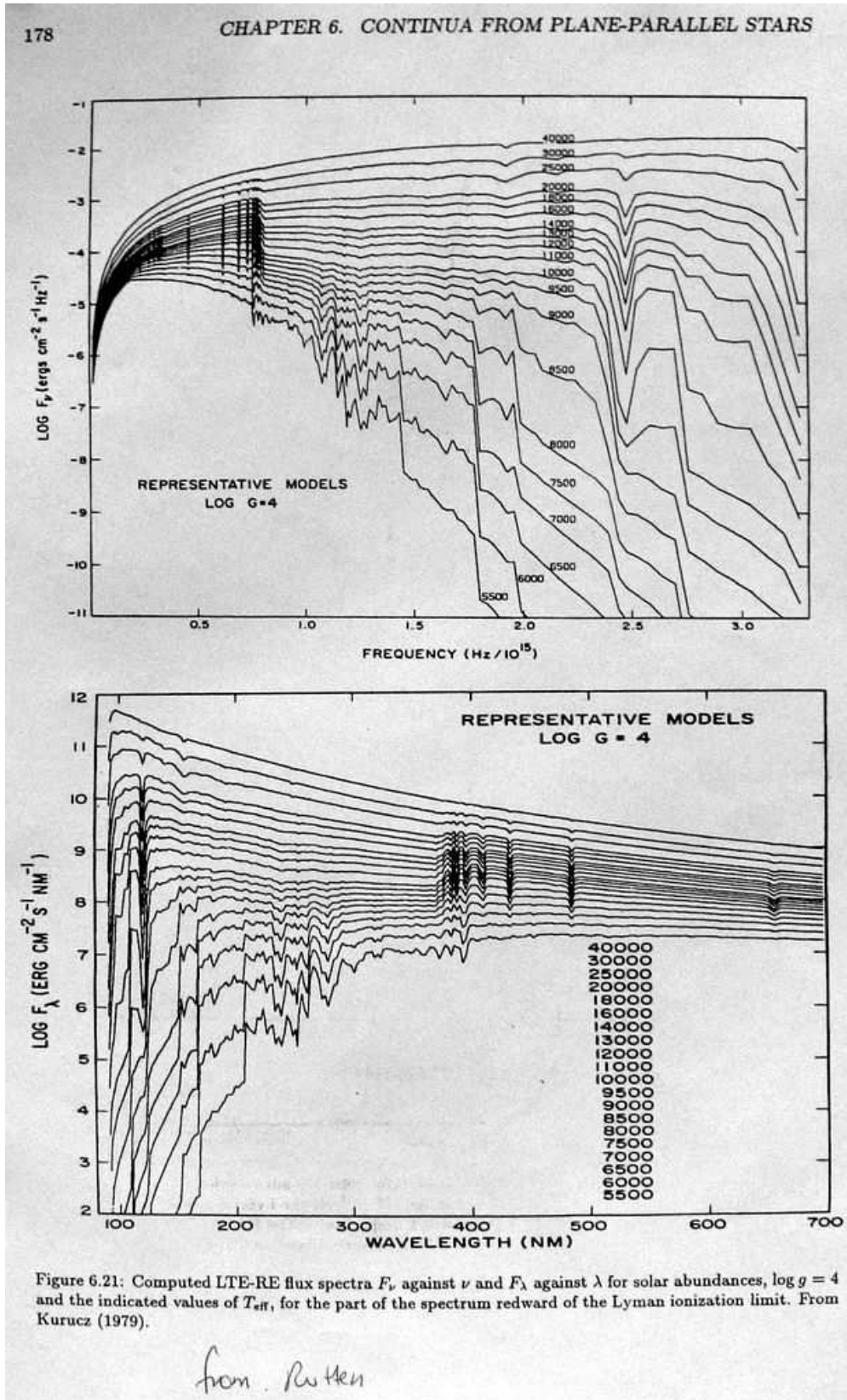


Fig. 4.— SEDs from the Kurucz model atmosphere grid for a wide range of  $T_{\text{eff}}$  Solar metallicity main sequence stars. Plots of  $F_\nu$  vs  $\nu$  and  $F_\lambda$  vs.  $\lambda$ . (Fig. 6.21 from Rutten)

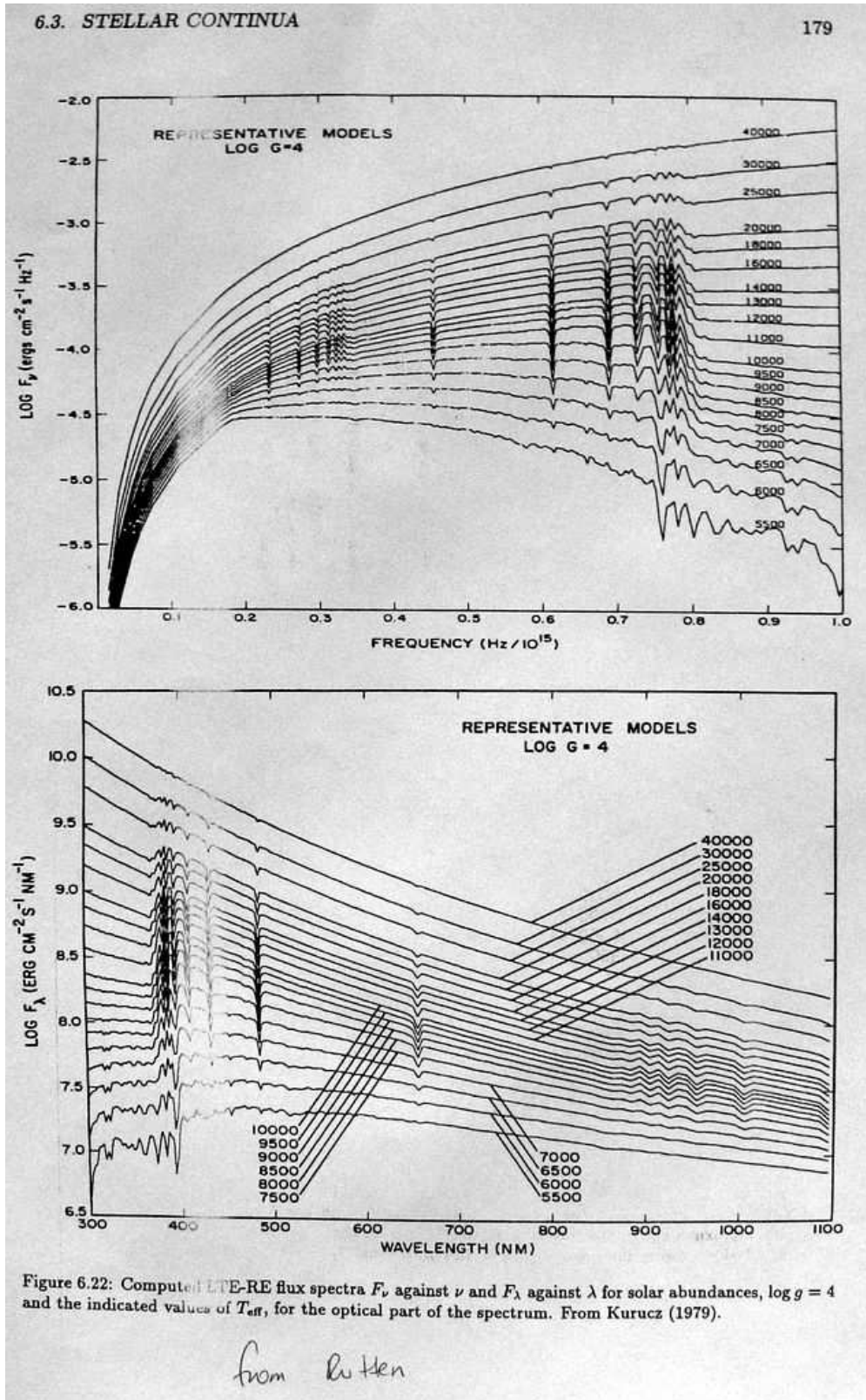


Fig. 5.— SEDs from the Kurucz model atmosphere grid for a wide range of  $T_{\text{eff}}$  Solar metallicity main sequence stars. Plots of  $F_\nu$  vs  $\nu$  and  $F_\lambda$  vs.  $\lambda$  for 0.3 to 1.1  $\mu$  wavelengths. (Fig. 6.22 from Rutten)

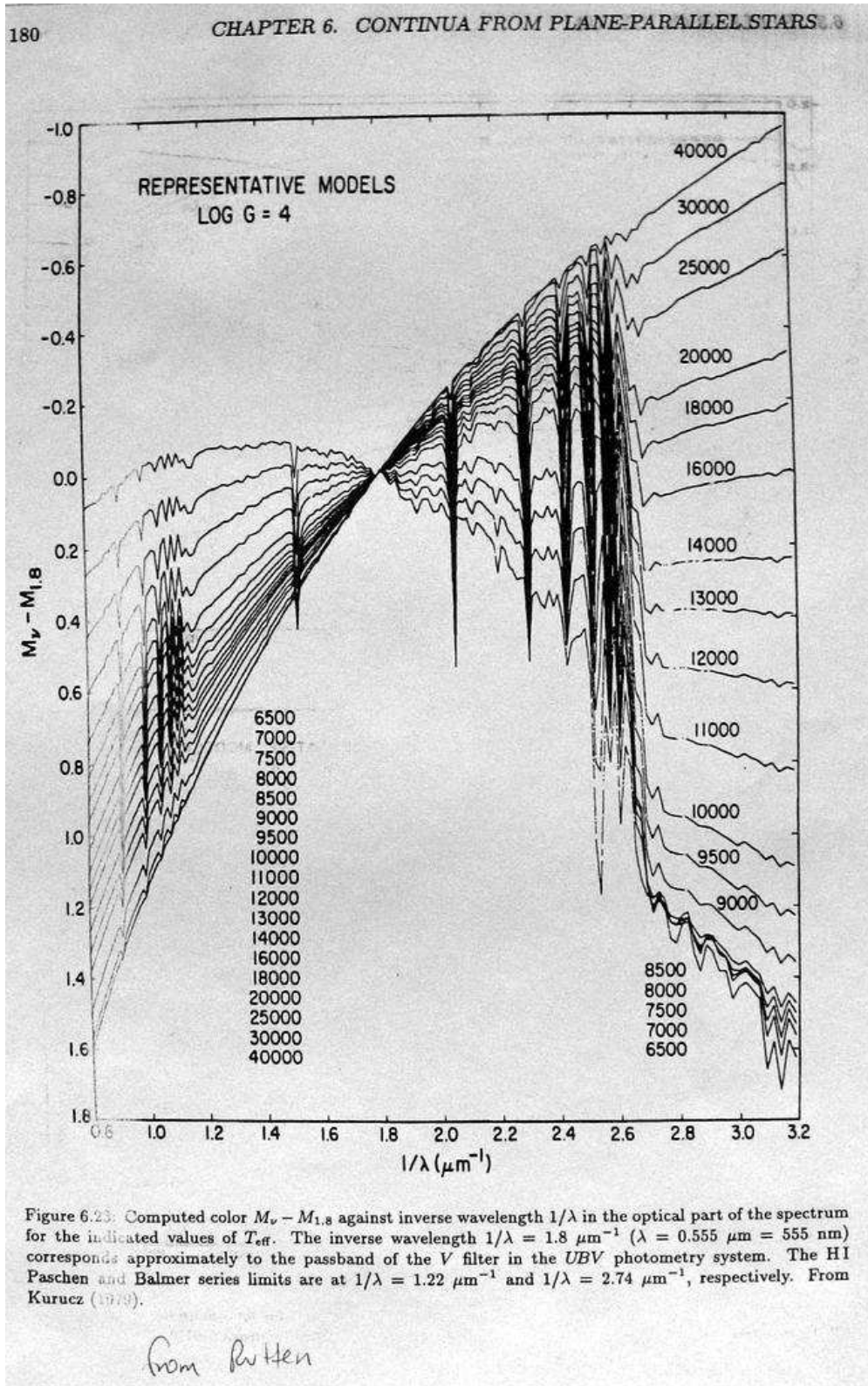


Fig. 6.— SEDs from the Kurucz model atmosphere grid for a wide range of  $T_{\text{eff}}$  Solar metallicity main sequence stars. These are all normalized to 0 at  $5500 \text{ \AA}$  ( $1/\lambda \text{ in } \mu = 1.8$ ). (Fig. 6.23 from Rutten)

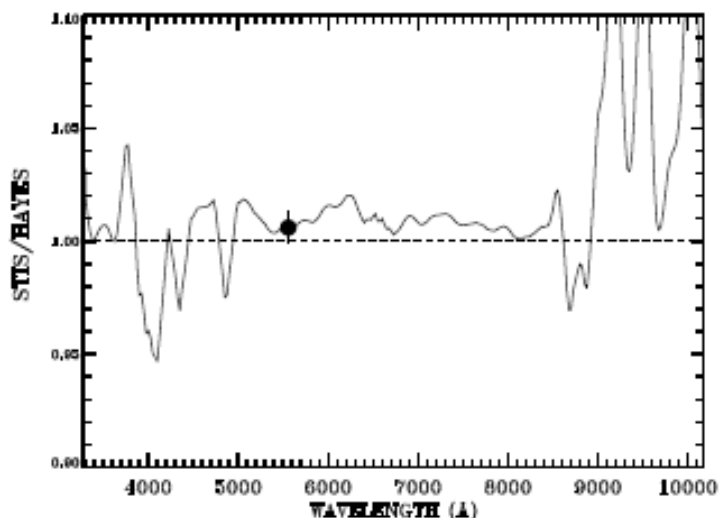


FIG. 2.— Ratio of the final STIS fluxes for Vega to those of Hayes (1985). The revised monochromatic flux of Megessier (1995) at 5556 Å is shown as the filled circle.

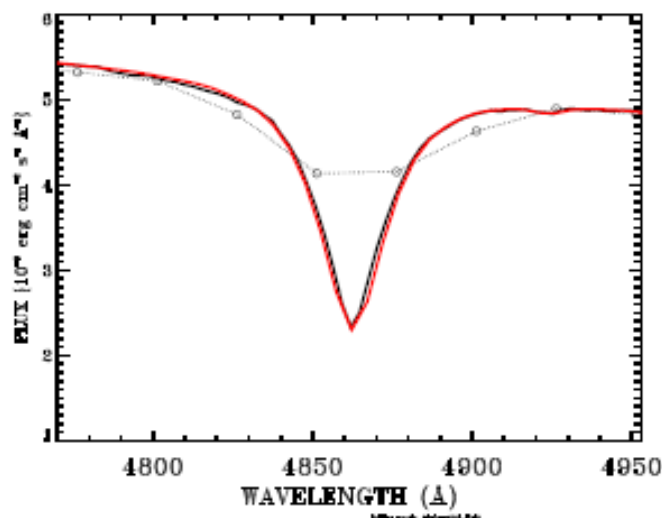


FIG. 3.— The  $H\beta$  spectral region. Solid line: final STIS flux, red line: Kurucz (2003)  $R = 500$  model scaled to  $3.46 \times 10^{-9} \text{ erg cm}^{-2} \text{ s}^{-1}$  at 5556 Å, dotted line with open circles: Hayes fluxes adjusted by 1.006 and wavelengths converted to vacuum to match STIS and the model.

Fig. 7.— Fig. 2 and 3 of Bohlin & Gilliland, 2004, AJ, 127, 3508. HST absolute spectrophotometry of Vega from far UV to IR. Top panel: Region of  $H\beta$ . Ratio of STIS fluxes from their work to those of Hayes (1985) in the optical range. Vertical range 0.9 to 1.10 (i.e. 10% flux errors) Bottom panel: STIS flux - solid line, Kurucz model - red line, Hayes (1985) fluxes slightly adjusted - open circles.

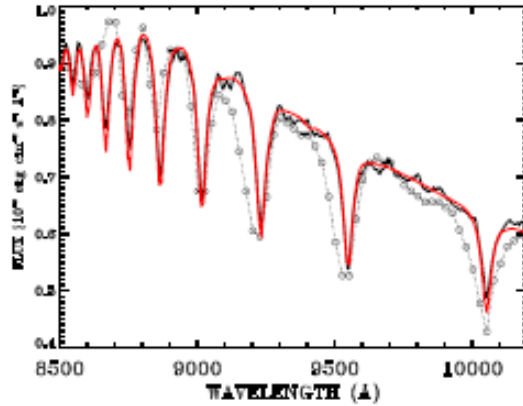


FIG. 4.— As in Figure 3 for the region of the H I Paschen lines, where the Hayes (1985) spectrophotometry differs the most from STIS and the Kurucz model. At these longest wavelengths of the STIS CCD data, the de-fringing technique leaves some residuals at the  $\sim 2\%$  level. The STIS data and  $R = 500$  model agree within the uncertainty of the de-fringing.

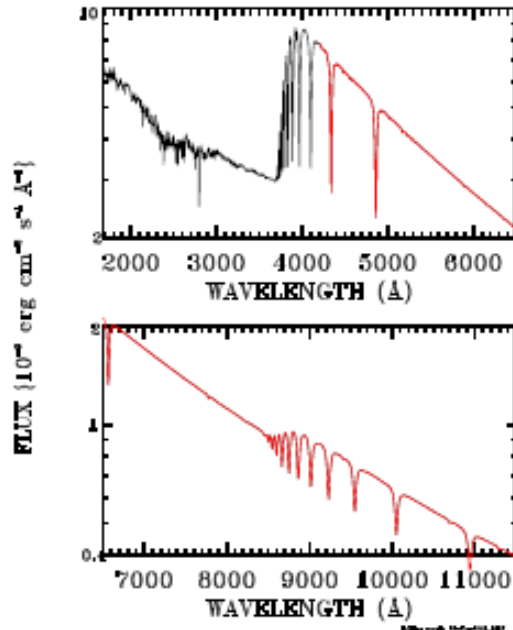


FIG. 5.— Absolute flux distribution of Vega as measured by STIS below 4200 Å and as determined by the Kurucz (2003)  $R = 500$  model at the longer wavelengths. Below 3000 Å the spectrum is dominated by metal line blanketing, while above 3000 Å, only the Balmer and Paschen lines of hydrogen are deeper than  $\sim 2\%$  at the STIS resolution of  $R \sim 500$ . The top panel shows the peak of the flux distribution down to  $2 \times 10^{-9}$  erg cm $^{-2}$  s $^{-1}$  Å $^{-1}$ , while the lower panel covers the next factor of five lower fluxes.

Fig. 8.— Fig. 4 and 5 of Bohlin & Gilliland, 2004, AJ, 127, 3508. HST absolute spectrophotometry of Vega from far UV to IR. Comparison of HST STIS spectra taken with a very wide slit (black line), Kurucz model atmosphere (red line), Hayes (1985) spectrophotometry over somewhat wider bandpass (open circles).

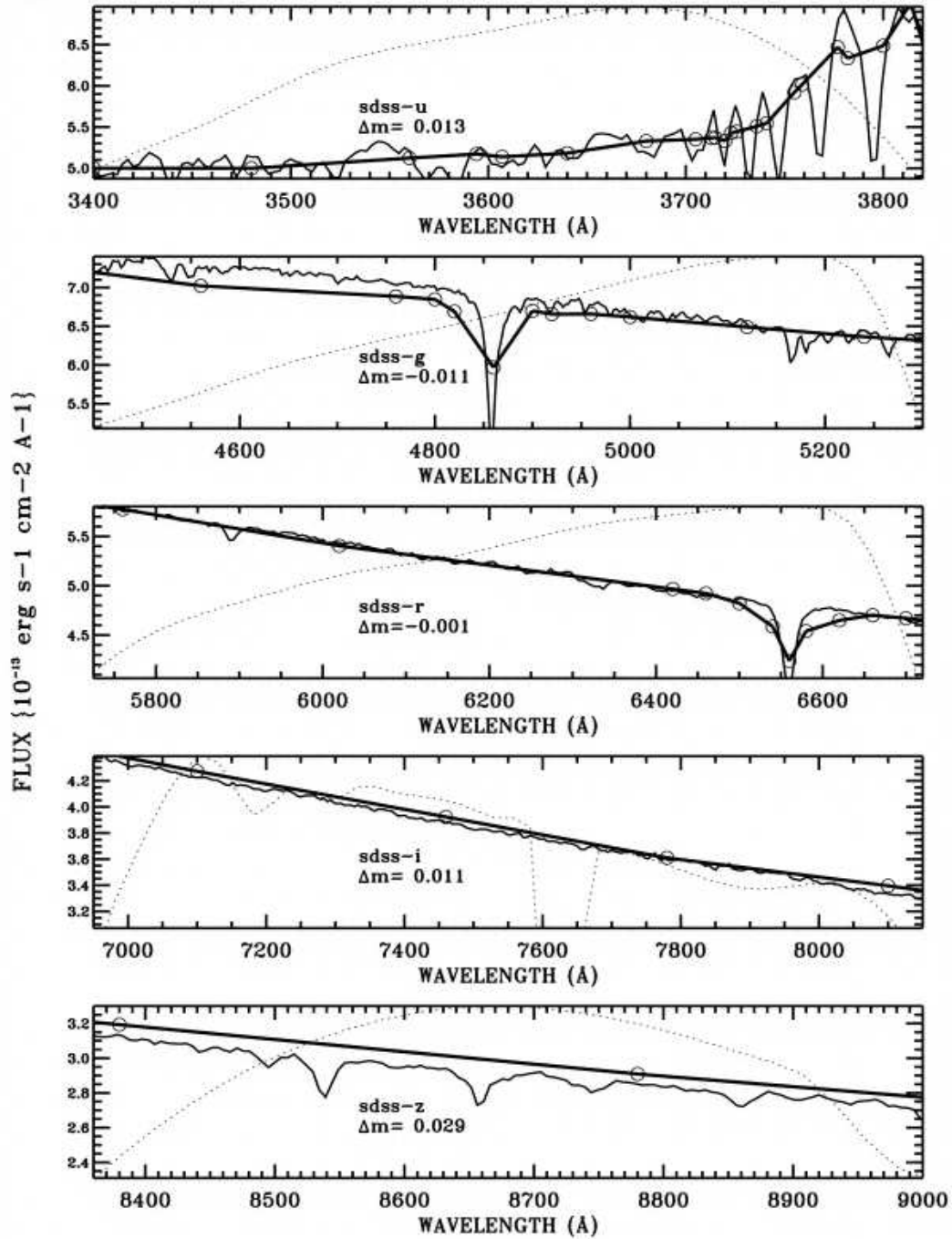


Fig. 9.— Fig. 2 of Bohlin & Gilliland, 2004, AJ, 128, 3053. Main standard used by SDSS BD+17 4708 (Vega is too bright). Fukugita et al 1996 (circles and heavy lines) - SDSS calibration STIS result - light thin line, models from Kurucz grid.

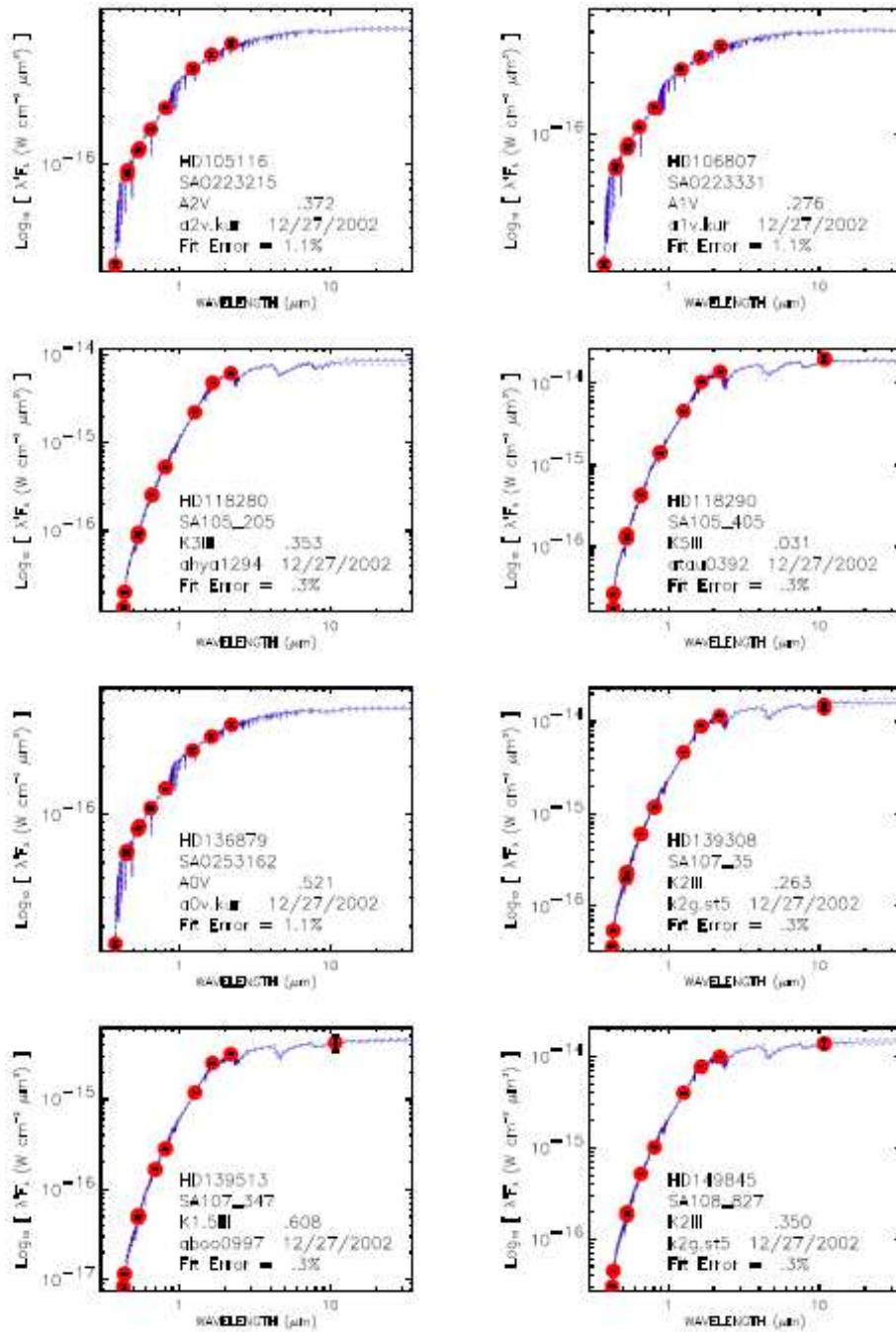
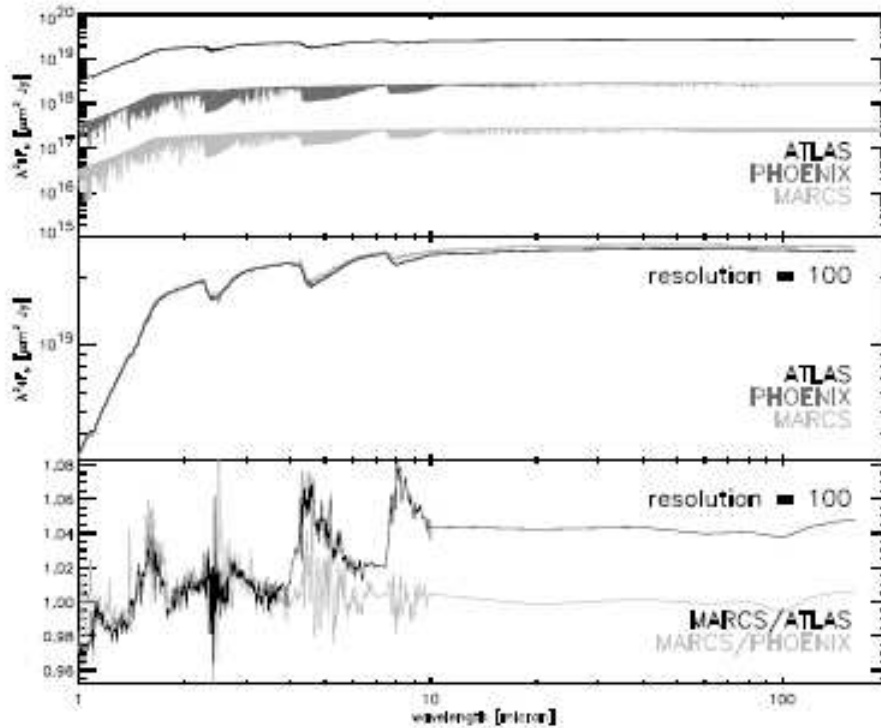
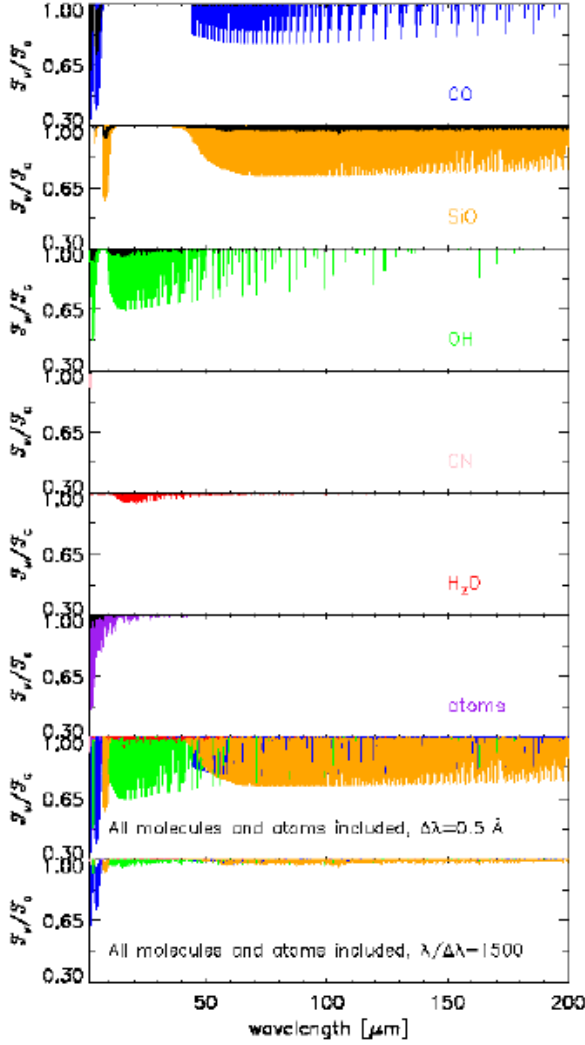


Fig. 10.— Fig. 7 of M.Cohen et al, 2003, AJ, 125, 2645 A montage of 8 supertemplates and models from 24 cool giants and 9 hot dwarfs is shown. Mean curves with 1 sigma boundaries. Normalizing photometry filled circles with 1 sigma error bars.



**Figure 6.** *Upper panel:* Comparison between the ATLAS, PHOENIX, and MARCS model spectra. The PHOENIX model is shifted downwards with a factor 10, and the MARCS model with a factor 100. *Middle panel:* Comparison between the ATLAS, PHOENIX and MARCS model spectra at a resolution of 100 for  $\lambda \leq 10 \mu\text{m}$ . At longer wavelengths, only the 8 wavelength points as given in the ATLAS models (at 20, 40, 60, 80, 100, 120, 140, and  $160 \mu\text{m}$ ) are retained. Difference between PHOENIX and MARCS model fluxes is barely visible. *Bottom panel:* Ratio between MARCS and ATLAS (black) and PHOENIX (gray) model fluxes.

Fig. 11.— Fig. 6 of Decin & Eriksson, astro-ph/0708.4120 (2007, A&A) Theoretical model atmosphere spectra used for calibration of far IR instruments. The vertical axis is predicted flux in units of  $\lambda^2 F_\nu$  (microns<sup>2</sup> Jansky)



**Figure 7.** Contribution of CO (blue), SiO (orange), OH (green), CN (pink), H<sub>2</sub>O (red), atoms (purple) to the 2 – 200 μm synthetic spectrum calculated from the atmosphere model with stellar parameters  $T_{\text{eff}} = 4320$  K,  $\log g [\text{cm/s}^2] = 1.50$ , mass  $M = 1.1 M_{\odot}$ ,  $[\text{Fe}/\text{H}] = -0.50$ , microturbulence  $\xi_t = 2 \text{ km s}^{-1}$ ,  $\epsilon(\text{C}) = 7.96$ ,  $\epsilon(\text{N}) = 7.61$ ,  $\epsilon(\text{O}) = 8.68$ ,  $\epsilon(\text{Mg}) = 7.33$ ,  $\epsilon(\text{Si}) = 7.20$ , and  $^{12}\text{C}/^{13}\text{C} = 7$ . The first six panels display the contribution at a resolution  $\Delta\lambda = 0.5 \text{ \AA}$  in color and at a medium resolution  $\lambda/\Delta\lambda = 1500$  in black. The total contribution to the full spectrum is shown in the seventh panel at the high resolution of  $\Delta\lambda = 0.5 \text{ \AA}$ , and in the bottom panel at the medium resolution of  $\lambda/\Delta\lambda = 1500$ . Note the lack of atomic absorption features for wavelengths longer than  $\sim 50 \mu\text{m}$ .

Fig. 12.— Fig. 7 of Decin & Eriksson, astro-ph/0708.4120 (2007, A&A) indicating the regions of strong absorption by various molecules and by atoms in the mid and far IR spectral regions.

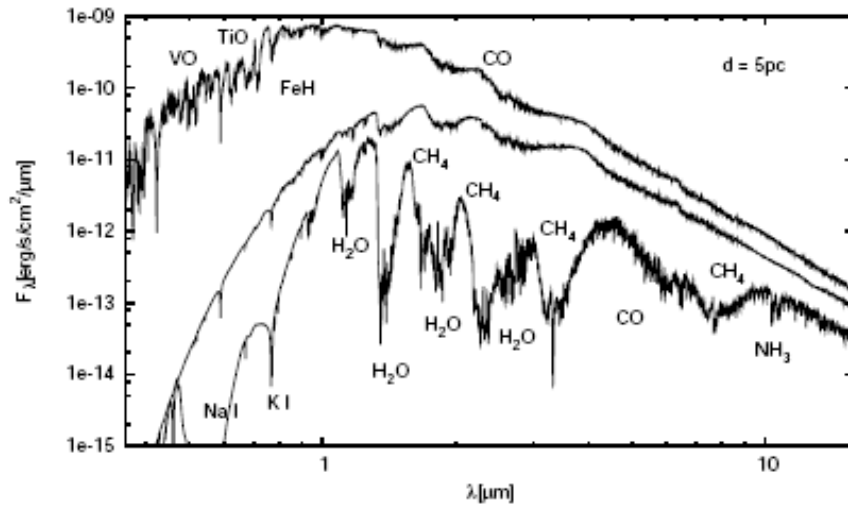


Fig. 2. Model spectra for the conditions typical of a VLM star ( $T_{\text{eff}} = 3\,500\text{ K}$ , top, with very little dust being formed), a young BD ( $T_{\text{eff}} = 1\,800\text{ K}$ , middle, with dust opacity included) and an older field BD ( $T_{\text{eff}} = 1\,000\text{ K}$ , bottom, without dust opacity). The most important absorption features are indicated.

Fig. 13.— Predicted spectra for brown dwarfs of varying temperatures and dust in their atmospheres. (Homeier, Allard, Hauschildt et al, 2003, in High Resolution IR Spectroscopy in Astronomy, Proceedings of an ESO Workshop)